STEM CELLS AND DEVELOPMENT
Volume 21, Number 2, 2012

DOI: 10.1089/scd.2010.0587

In Vitro Imaging of Angiogenesis Using Embryonic Stem Cell-Derived Endothelial Cells

Jia Li[1,2] and Heidi Stuhlmann[1]

Angiogenesis is an important event during developmental processes, and it plays a key role in neovascularization. The development of an in vitro model that can be used for live imaging of vessel growth will facilitate the study of molecular and cellular mechanisms for the growth of blood vessels. Embryonic stem cells (ESCs) are considered to be a novel renewable source for the derivation of genetically manipulable endothelial cells (ECs). To derive green fluorescence protein (GFP)-expressing ECs, we used a transgenic ESC line in which a GFP reporter was driven by the endothelial-specific promoter fetal liver kinase 1. ESC-ECs were isolated from 11-day embryoid bodies by fluorescence-activated cell sorting. Embedding the aggregated ESC-ECs in a 3-dimensional collagen gel matrix resulted in ESC-EC migration out of the aggregates and coalescence into a capillary network. Time-lapse microscopy revealed EC migration, proliferation, lumen formation, and anastomosis to other capillary vessels during this process, which were reminiscent of angiogenic processes. Vascular endothelial growth factor plays major roles in the induction of ESC-EC angiogenesis in vitro. Blockage of the β1 integrin subunit severely impaired ESC-EC survival and migration. We demonstrate that our in vitro ESC-EC angiogenesis model represents a high-resolution dynamic video-image system for observing the cellular events underlying angiogenic cascades. We also consider this model as an image screening tool for the identification of pro-angiogenic and anti-angiogenic molecules.

Introduction

Angiogenesis, the development of new blood vessels from preexisting ones, is a critical event during developmental and pathological vascular development [1]. Angiogenesis is a morphogenic process that involves the stimulation of normally quiescent endothelial cells (ECs) to undergo basement membrane degradation, invasion, migration, proliferation, lumen formation, and differentiation [2,3]. Recently, advances in the understanding of angiogenesis have been translated to the development of drugs targeting angiogenesis in conditions such as cancer or the induction of neovascularization [4]. Accordingly, numerous in vivo and in vitro angiogenesis models have been developed for the identification of anti-angiogenic or pro-angiogenic compounds. Current in vivo systems, such as the chick chorioallantoic membrane assay [5–7], corneal neovascularization assay [8–10], matrigel plug assay [11,12], and transgenic zebrafish models [13–15] are limited by the species used, organ sites, administration of the test substances, and lack of quantitative analysis [16]. Ex vivo models, such as rat aortic ring [17], chick aortic arch [18], and vena cava explants [19], provide excellent recapitulation of various stages of angiogenesis; however, these cultures contain multiple cell types, and reliable transfection is problematic. Therefore, numerous in vitro angiogenesis assays have been developed, despite the fact that they are incapable of modeling all of the components of the angiogenic cascade. Recently, an in vitro tube formation assay, which involves plating ECs or EC aggregates onto or into a 3-dimensional (3D) gel matrix, was extensively used to study pro-angiogenic or anti-angiogenic molecules, as they could model EC adhesion, migration, protease activity, and lumen/tube formation. The most commonly used ECs for this assay are human umbilical vein endothelial cells, which are easily isolated and have been successfully cultured since 1973 [20–23]. However, utilizing these macrovascular ECs are far from ideal, as angiogenesis commonly involves the microvasculature rather than the macrovasculature [16,24,25]. Currently, there is no available in vitro assay that permits prolonged high-resolution imaging of EC behavior in a non-invasive manner. This hinders the detailed analysis of which molecules govern the proper guidance of growing vessels or the interactions of molecules that are required for blood vessel morphogenesis. Therefore, it would be beneficial to devise a new in vitro system that allows continuous imaging of the behavior of wild-type or mutated ECs during angiogenesis.

Embryonic stem (ES) cells are characterized by their capacity for prolonged undifferentiated proliferation in culture,

[1]Department of Cell and Developmental Biology, Weill Medical College of Cornell University, New York, New York.
[2]Med-X-Renji-Clinical Stem Cell Institute, Renji Hospital, Shanghai Jiaotong University Medical College, Shanghai, China.

while retaining the potential to differentiate into all 3 germ layer cells both in vivo and in vitro. In culture, embryonic stem cells (ESCs) can differentiate into ECs through successive maturation steps, as manifested by endothelial-specific markers such as fetal liver kinase 1 (Flk 1), platelet endothelial cell adhesion molecule, vascular endothelial (VE)-cadherin, and von Willebrand factor. ESC-ECs express endothelial-specific markers and have been found to form capillary structures in vitro and in vivo [26,27]. In addition, the relative ease by which ESCs can be genetically manipulated has made them a powerful tool to target endogenous genes, and this can facilitate the manipulation of gene expression in ESC-ECs. For this reason, ESCs are an ideal renewable source for the generation of genetically manipulable microvascular ECs. To observe developing vasculature, we used a transgenic ESC line in which a green fluorescent protein (GFP) reporter was driven by the EC-specific promoter Flk 1, which makes the ECs isolated from this ESC line express GFP. We searched for conditions that promoted angiogenesis and maintained the long-term GFP expression of ESC-ECs throughout the entire morphogenetic processes. Finally, we show that our established system could mimic angiogenic stimuli-induced angiogenesis and, therefore, can be applied for high-resolution live cell imaging of EC behavior during an angiogenic cascade in vitro.

Materials and Methods

Culture and maintenance of mouse ESCs

The Flk 1-GFP-targeted R1 ESCs were generated by knocking in a GFP reporter in-frame into the start codon of exon 1 of the Flk 1 genomic locus (gift from Dr. Janet Rossant, Mount Sinai Hospital, Samuel Lunenfeld Research Institute, Toronto, Canada). Wild-type R1 ESCs were obtained from the mouse genetics core facility at Memorial Sloan-Kettering Cancer Center (New York, NY). ESCs were grown on mitomycin-C-treated feeder cells in a high-glucose Dulbecco's modified Eagle's medium (Invitrogen) supplemented with 15% ESC-qualified fetal bovine serum (FBS; Invitrogen), 100× penicillin/streptomycin (Invitrogen), 2 mM L-glutamine (Invitrogen), 100× ESC-qualified nucleotides (Millipore), 100× MEM nonessential amino acids (Invitrogen), 0.05 mM 2-mercaptoethanol (Sigma), and 5×10^5 U leukemia inhibitory factor (ESGRO) at 37°C in 5% CO_2.

In vitro differentiation of ESCs

For the in vitro differentiation of ESCs into embryonic bodies (EBs), subconfluent Flk $1^{GFP/+}$ or wild-type R1 ESCs were trypsinized and diluted with differentiation media (DM) into 8.3×10^4 cells/mL cell suspensions. To make hanging drops, 100× 30 μL aliquots of ESC suspension were plated on the inner side of the bottom of a 150-mm uncoated bacteriological Petri dish (Fisher). The DM contains ESC media without leukemia inhibitory factor and 20% FBS. On day 2, EBs formed and were suspended in DM for another 1–2 days. On day 3 or 4, these EBs were seeded on 0.2% gelatin-coated 60 mm tissue culture dishes (for fluorescence-activated cell sorting) or collagen type I-coated 35 mm glass bottom dishes (for morphological analysis and live imaging). DM with 50 ng/mL vascular endothelial growth factor $(VEGF)_{164}$ (R&D systems) was then added after 12 h of seeding. All cultures were maintained at 37°C in 5% CO_2.

Isolation of ESC-ECs

Day 11 Flk $1^{GFP/+}$ or wild-type R1 ESC-derived-EBs were dissociated with collagenase/dispase (Roche) containing 10% FBS and 200 U/mL DNAse I (Invitrogen) for 1.5 h in a 37°C incubator. Phosphate-buffered saline (PBS) was added to the plates to stop collagenase activity. After pipetting up and down several times until no obvious clumps appeared, cell suspensions were washed through a G20 syringe and then filtered through a 40 μm strainer (Falcon) to create single-cell suspensions. Approximately 1×10^7 Flk $1^{GFP/+}$ R1 ESC-derived EB cells and control wild-type R1 ESC-derived EB cells were subjected to cell sorting. Every 3,000 Flk 1^+ cells were isolated using a BD FACStar™ Plus flow cytometer (BD Biosciences) and plated into each well of a 96-well Costar ultra-low attachment dish (Fisher) in 2× EC medium with 0.25% (v/w) methylcellulose and 100 ng/mL $VEGF_{164}$ (R&D systems). EC medium contained α-MEM (Invitrogen) supplemented with 10% FBS and 5×10^{-5} M 2-mercaptoethanol.

In vitro angiogenesis assay

To make 1.5 mg/mL type I collagen gel solution, a 3 mg/mL type I collagen gel solution was prepared from 3.78 mg/mL rat tail type I collagen (BD Biosciences) on ice following the manufacturer's instructions. Half of the 2× EC medium with 100 ng/mL $VEGF_{164}$ and half of the 3 mg/mL type I collagen gel solution were added in a mixture at 0°C.

To make the gel-aggregate-gel sandwich for in vitro angiogenesis, 75 μL of 1.5 mg/mL collagen gel solution was added to each well of a 96-well glass-bottom plate (MatTek) on ice and was rapidly transferred into a 37°C incubator to allow polymerization for 30 min. Aggregates were seeded on top of the polymerized type I collagen gel and allowed to adhere for 15 min at 0°C. Seventy-five microliters of 1.5 mg/mL gel solution was added on top of the aggregates at 0°C. After polymerization for 30 min at 37°C, 100 μL of EC medium containing 50 ng/mL $VEGF_{164}$ was pipetted on top of the gel. Sometimes, monoclonal antibodies against integrin β1 chain (BD Pharmingen™ Cat. no. 555002) were added into the culture at a concentration of 50 μg/mL. All cultures were placed at 37°C in 5% CO_2 at 100% humidity.

Time-lapse live cell imaging

To prepare for time-lapse live cell imaging, a 2 mL gel sandwich with 10 aggregates was prepared in a 35 mm glass-bottom dish following the methods described above. Three days later, time-lapse conditions were established. In general, a temperature-controlled chamber was set at 37°C with a continuous 5% CO_2 infusion and allowed to equilibrate before inserting the 35 mm glass-bottom dish. GFP was excited at 480 nm. Stacks of images were taken with a Zeiss LSM 5 LIVE laser scanning confocal microscope every 10 min with a slice number between 50 and 90. Movies were processed using LSM software (version 4.0.0.241, Zeiss).

Immunofluorescence staining

Anti-Flk 1 immunofluorescence staining was performed on the microwell of 35 mm glass-bottom dishes. Day 11 wild-type ESC-derived EBs were fixed with 4% paraformaldehyde

for 15 min at room temperature. After rinsing in PBS, EBs were permeabilized with 0.2% Triton-X 100 in PBS for 15 min. After several washes, EBs were incubated with blocking solution [3% rabbit serum (heat inactivated; Sigma) and 1% BSA (Sigma) in PBS] for 1 h at 37°C, and then incubated with rat anti-mouse Flk 1 monoclonal antibody (1:50 dilution; BD Pharmingen) in a humid chamber at 4°C overnight. The next day, after several washes, EBs were incubated with FITC-conjugated goat anti-rat IgG polyclonal antibody (Abcam) for 2 h. EBs were mounted in aqueous medium and observed under a Zeiss LSM 5 LIVE laser scanning confocal microscope. FITC was excited at 480 nm.

RNA extraction and reverse transcription–polymerase chain reaction

Total RNA was isolated from undifferentiated ESCs, day 4, 6, 8, 11, and 13 Flk 1^+ cells, using Trizol (Invitrogen). Primer sequences for specific genes (*Flk 1*, *Cd31*, *VE-cadherin*, *Scl/Tal 1*, *Oct 4*, and *Gapdh*) are listed in Table 1. Unless stated otherwise, all experiments were performed in triplicate.

Statistical analyses

Data were analyzed by a 2-tailed Student *t*-test using SAS V8 software (SAS Institute).

Results

In vitro differentiation of Flk $1^{GFP/+}$ ESCs

To develop a reliable system to purify mature ECs from ESCs, we used a transgenic Flk $1^{GFP/+}$ R1 ESC line that expresses GFP under the endogenous EC-specific Flk 1 promoter. To determine whether vasculogenesis and angiogenesis in the ESC-derived EBs were affected by the insertion of a transgene into the Flk 1 genomic locus, we performed a time-course observation of the GFP-expressing cells during EB differentiation. On differentiation day 4, a small portion of EB cells started to express GFP. On differentiation day 6, a sheet of round-shaped cells appeared in the periphery of the flattened EBs (Fig. 1A, a) that moved back and forth with frequent cell–cell interactions (Supplementary Movie S1; Supplementary Data are available online at www.liebertonline.com/scd). On differentiation day 8, GFP-expressing ECs generated extensive filopodial extensions and migrated to the target vessel by gliding on a 2-dimensional (2D) substratum (Supplementary Movie S2). In the end, the cells coalesced to form a primitive vascular plexus (Fig. 1A, b). On differentiation day 11, the primitive vascular plexus was remodeled into a highly branched vascular network (Fig. 1A, c). Morphogenesis of the GFP-expressing cells during EB differentiation recapitulates vasculogenesis and early angiogenesis in vitro. The entire morphogenic progress is similar to that of Flk 1^+ cells in the wild-type R1 ESC-derived EBs (Fig. 1B, d–f).

To further analyze whether heterozygous Flk 1 expression affects EC lineage determination during EB differentiation, flow cytometry was performed based on GFP expression in Flk $1^{GFP/+}$ EBs or by using an antibody against Flk 1 in wild-type EBs (Fig. 1C). The number of Flk 1^+ cells consistently increased in the first 11 days, whereas it decreased on day 13 in both Flk $1^{GFP/+}$ and wild-type EBs (Fig. 1D). However, there was a modest reduction in the number of Flk 1^+ cells in Flk $1^{GFP/+}$ EBs over time, as compared with the wild-type EBs. This result indicates a similar trend for the differentiation of the EC lineage in both the Flk $1^{GFP/+}$ EBs and the wild-type EBs, although the former had a moderately reduced frequency.

In vitro characterization of Flk 1^+ cell fractions

To characterize the Flk 1^+ cell fractions in various developmental stages, Flk 1^+ cells were sorted from day 4, 6, 8, 11, and 13 EBs using fluorescence-activated cell sorting. The potential expression of several endothelial-specific genes and markers for undifferentiated ESCs was analyzed in the undifferentiated ESCs and the purified Flk 1^+ cells (Fig. 2). Reverse transcription–polymerase chain reaction results demonstrated expression of *Flk 1* and *Cd 31* during all stages of differentiation. Expression of *VE-cadherin* appeared by day 6. von Willebrand factor mRNA was detected by day 8. Expression of the hematopoietic lineage marker *Scl/Tal 1* was detected at high levels before day 6, but progressively decreased upon maturation of hemangioblasts to ECs on days 8, 11, and 13. As expected, ESCs did not express any of the above-mentioned markers, except for a low mRNA level of CD31. The ESC marker *Oct 4* was expressed in undifferentiated ESCs, with no expression at any stage in Flk 1^+ cells. Taken together, Flk 1^+ cell fractions differentiated into more

Table 1. Oligonucleotide Primer Sequences Used for Reverse Transcription–Polymerase Chain Reaction

Gene name	*Sequence*	*GenBank no.*
Flk 1	5′ AGCAACACACAGCGAGCATC 3′ 5′ TAAGTAAGTTGATAGGTTTC 3′	NM_010612
CD31	5′ GCAAAGAGTGACTTCCAGAC 3′ 5′ GCAAAGAGTGACTTCCAGAC 3′	NM_008816
VE-cadherine	5′ CAGTACACATTCTACATTGA 3′ 5′ TCAATGTAGAATGTGTACTG 3′	NM_009868
vWf	5′ GCAGAAACAGCCTATGGATC 3′ 5′ GACAGCTTAACCAGTAGCCG 3′	NM_011708
Scl/Tal 1	5′ CGGTCTGGTGTATCGCAGTG 3′ 5′ AAGATGTAATTCTCTATTTG 3′	U01530
Oct 4	5′ AAGGAGCTAGAACAGTTTGC 3′ 5′ ACCATACTCGAACCACATCC 3′	NM_013633
Gapdh	5′ GCCCATCACCATCTTCCAG 3′ 5′ TGAGCCCTTCCACAATGCC 3′	NM_008084

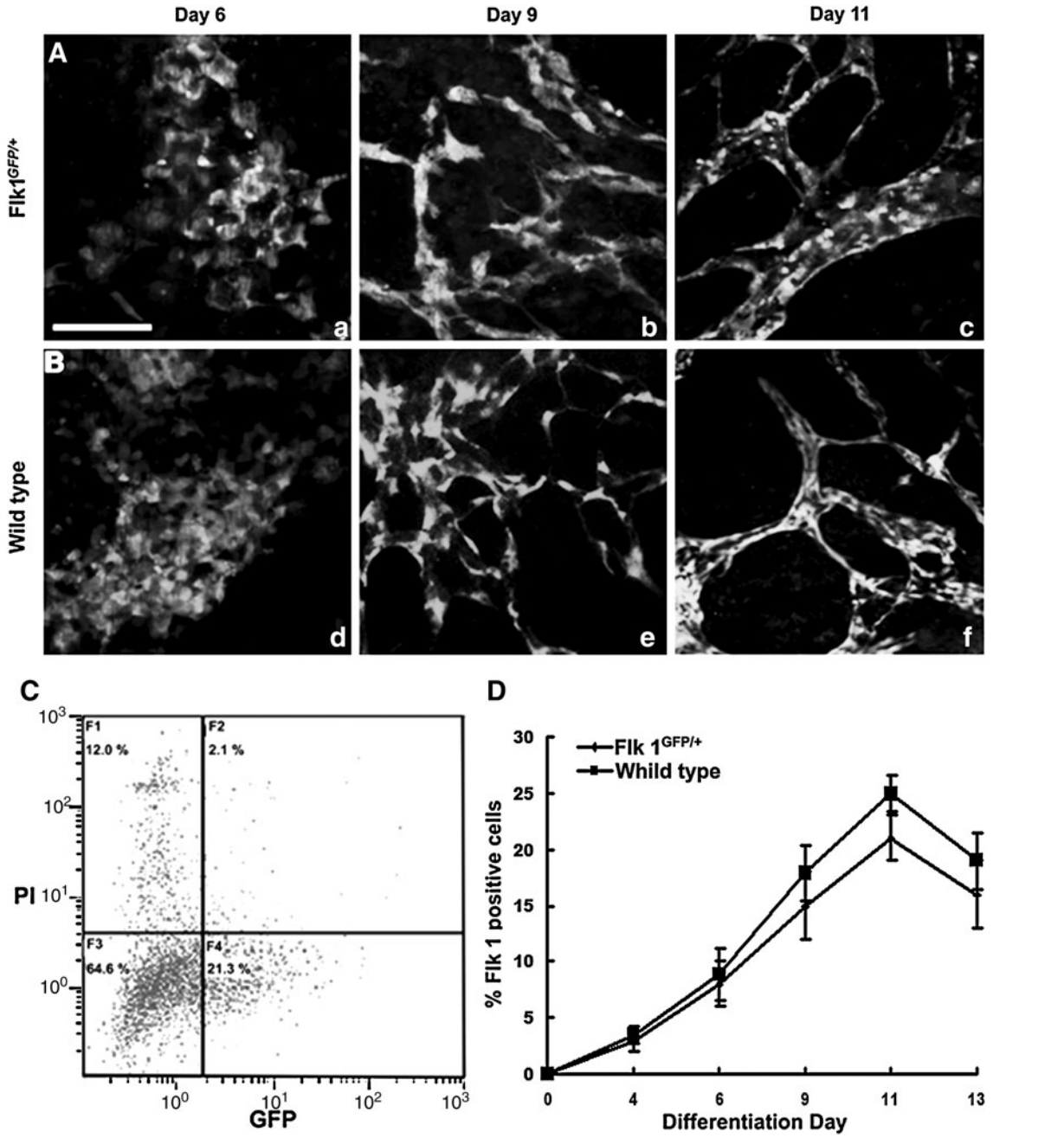

FIG. 1. Vascular development in Flk $1^{GFP/+}$ and wild-type ESC-derived EBs. **(A)** Flk $1^{GFP/+}$ EBs on day 6 **(a)**, day 9 **(b)**, and day 11 **(c)**. **(B)** Immunofluorescence staining for Flk 1 in wild-type EBs on day 6 **(d)**, day 9 **(e)**, and day 11 **(f)**. **(C)** Flow cytometry performed on day 11 Flk $1^{GFP/+}$ EB cells. **(D)** Fluorescence-activated cell sorting analysis of the percentage of Flk 1^{+} cells in both the Flk $1^{GFP/+}$ EBs and wild-type EBs. Scale bar: 200 μm. Flk 1, fetal liver kinase 1; ESC, embryonic stem cell; EBs, embryonic bodies.

mature ECs from day 8 onward. Additionally, because day 11 EBs gave rise to the largest number of Flk 1^{+} cells in EB differentiation, ECs were routinely derived from day 11 EBs for the following experiments.

ESC-EC spheroids suspended in a 3D collagen matrix form a capillary network

In an attempt to establish an ESC-EC in vitro angiogenesis model, we embedded the single-suspended GFP-expressing ESC-ECs in a 3D collagen matrix; however, massive apoptosis occurred after 24 h (data not shown). It has been reported that the formation of cell aggregates increases intracellular contacts and reduces cell tensile stresses, resulting in cessation of cell growth and facilitation of tubular network formation [28,29]. Therefore, we induced ESC-EC aggregate formation in a nonadhesion 96-well plate with α-MEM media containing methylcellulose. Single aggregates contained 3,000 ESC-ECs with sizes ranging from 250 to 300 μm, and each was formed in a single well of a 96-well plate within 18 h.

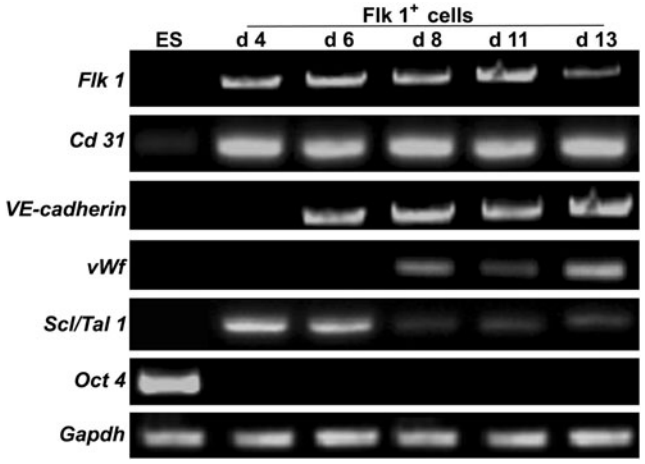

FIG. 2. Expression profiles of EC-specific genes in purified Flk 1^+ cells over time. Expression levels of *Flk 1, Cd 31, VE-cadherin, vWf, Scl/Tal 1,* and *Oct 4* were detected using reverse transcription–polymerase chain reaction on the undifferentiated ESCs (ES) and Flk 1^+ cells derived from day 4 (d 4), 6 (d 6), 8 (d 8), 11 (d 11), and 13 (d 13) EBs. GAPDH mRNA provided a positive control for RNA quantity. EC, endothelial cell.

Initially, we simply plated aggregates onto collagen type I-coated plates. In the presence of 50 ng/mL VEGF, GFP-expressing cord-like ECs appeared in the flattened aggregates after 24 h (Fig. 3D), whereas the ECs had lost GFP expression by 48 h (Fig. 3F). An increase in VEGF concentration (as high as 100 ng/mL) could not alleviate the loss of GFP expression in these ECs. A cell death assay indicated ESC-EC apoptosis during this process (data not shown). However, when we plated another 3D collagen gel matrix on top of the 2D culture, ECs migrated out and formed cord-like structures by 24 h (Fig. 4F), which could be maintained longer than 48 h (Fig. 4G). However, no further development was observed in this culture.

Several aggregates were inserted into a 3D collagen I gel sandwich that contained 50 ng/mL VEGF. As shown in Fig. 5, ESC-ECs from the aggregates rearranged into networks of capillary-like structures over a period of days. On day 2, GFP-expressing ECs on the aggregate surface migrated out, invaded the collagen matrix, and formed cord-like structures that had few luminal compartments (Fig. 5B). ECs in the center of the aggregate remained as a cell mass (Fig. 5B, asterisk). On day 3, cord-like ECs assembled into a vascular network (Fig. 5C), whereas ECs in the aggregate center had disappeared. By day 4, the vascular network was remodeled into a complex web of interconnected capillaries (Fig. 5D). These capillaries (Fig. 5E, arrowhead) contained lumens (Fig. 5E, asterisk) that were lined by 5–6 flattened ECs (Fig. 5E, arrows). Some of the lining ECs had abluminal filopodial extensions (Fig. 5E, twin arrows). On day 7, aggregates began to fall apart, and capillaries progressively collapsed (Fig. 5F).

VEGF specifically induces ESC-EC angiogensis

The above experiments indicated that when aggregates were embedded in the 3D collagen gel, ECs migrated out and underwent a series of morphogenetic processes leading to capillary network formation. We described these aggregates as angiogenic aggregates (Fig. 6A, b). However, in some cases, GFP-expressing ECs stayed inside the aggregates during the entire period. We describe these aggregates as nonangiogenic aggregates (Fig. 6A, d). These 2 phenotypes are easily distinguishable under a fluorescence microscope and are considered to be angiogenic criteria in our system.

We also asked whether the 2 observed phenotypes were determined by angiogenic growth factors (GFs). VEGF and

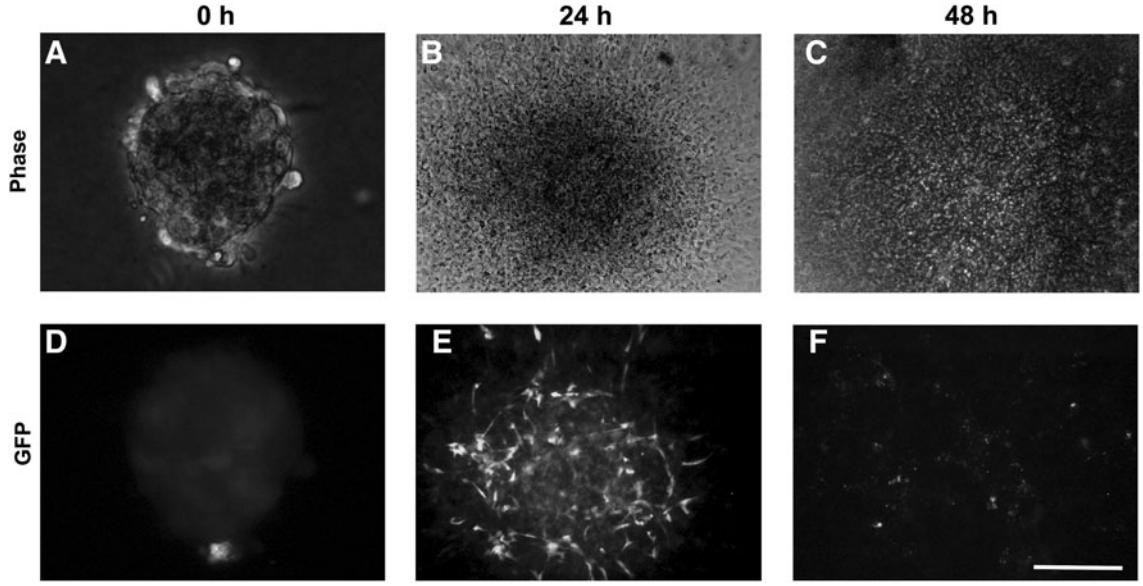

FIG. 3. ESC-EC aggregates on a collagen I-coated 2D substratum. **(A–C)** Bright-field ESC-EC aggregates at the indicated time. **(D–F)** The development of GFP-expressing ESC-ECs over time. **(E)** The appearance of GFP-expressing cord-like ESC-ECs after 24 h of plating. **(F)** GFP-expressing cells disappear after 48 h. Scale bar, 200 μm. GFP, green fluorescent protein.

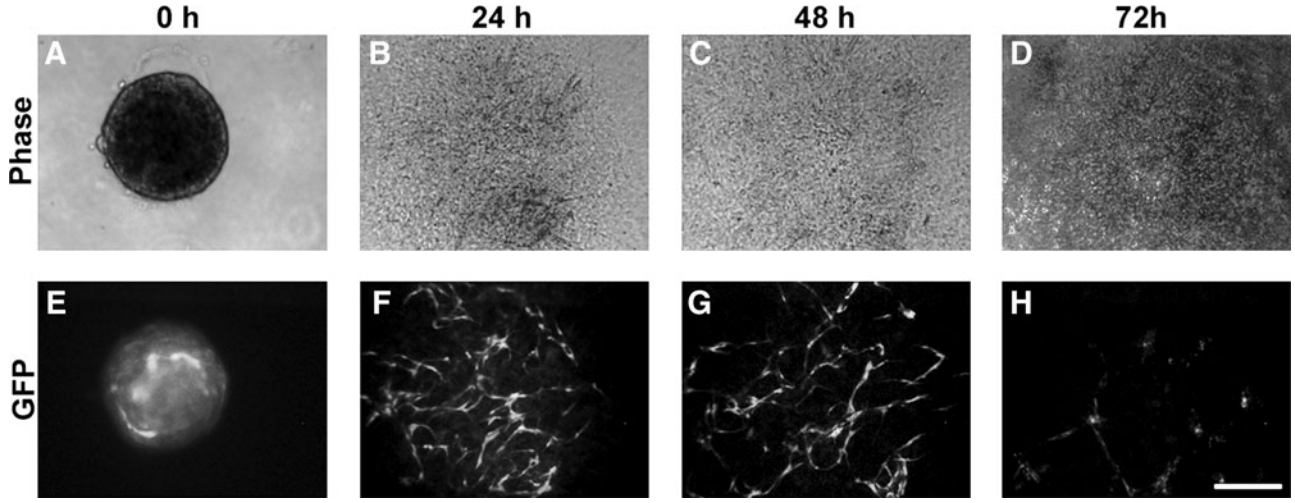

FIG. 4. ESC-EC aggregates on a collagen I-coated 2D substratum and beneath a collagen I gel matrix. **(A–D)** Bright-field ESC-EC aggregates at the indicated time. **(E–H)** The development of GFP-expressing ESC-ECs over time. **(F, G)** The appearance of GFP-expressing cord-like ESC-ECs after 24 h. **(H)** Collapse of GFP-expressing cord-like ESC-ECs at 72 h. Scale bar, 200 μm.

fibroblast growth factor 2 (FGF2), 2 factors that have been shown to play major roles in angiogenesis both in vitro and in vivo [30–34], were added to the culture. The effect of angiogenic GFs was evaluated based on the percentage of angiogenic aggregates among the total aggregates. As shown in Fig. 6B, 86% ± 8% of EC aggregates displayed angiogenic growth when both VEGF (100 ng/mL) and FGF2 (100 ng/mL) were present. None of the aggregates could undergo angiogenic growth without angiogenic GFs. VEGF or FGF2 alone was found to elicit a dose-dependent stimulation of angiogenesis. VEGF alone could account for around 95% of the response induced by both factors. In the presence of 100 ng/mL VEGF, 82% ± 4% of the aggregates displayed angiogenic growth. Nevertheless, FGF2 had a minor contribution to the induction of angiogenesis. At most, 23% ± 3% of the angiogenic aggregates were induced when we increased the concentration of FGF2 to the maximum dose.

β1 integrin blocking antibody inhibits ESC-EC angiogenesis

Cell surface integrins are the major receptors for the extracellular matrix and have been implicated in angiogenic processes, such as extracellular matrix remodeling, EC migration, proliferation, and the functional maturation of new ECs into mature blood vessels [35–37]. α1β1, α2β1, and α3β1 integrins are receptors for type I collagen [38,39]. To evaluate whether β1 integrin blockade exerts an effects on inhibition of ESC-EC angiogenesis in vitro, an β1 integrin blocking antibody was added into the aggregates embedded 3D collagen matrix in the presence of 100 ng/mL VEGF. After 72 h of β1 integrin inhibition, the appearance of the angiogenic aggregates decreased by 64% in compared with IgG control (Fig. 7A). Additionally, around 5% of the aggregates showed modest angiogenic growth upon anti-integrin β1 treatment for 72 h (Fig. 7B). However, the average vascularized area of these aggregates was dramatically decreased by 90% (Fig. 7C) and ESC-EC survival was significantly reduced by 43% (Fig. 7D), as compared with IgG control.

Time-lapse imaging of cellular events during capillary network formation

To evaluate the utility of the model for studying the cellular mechanism underlying angiogenesis in vitro, we performed time-lapse microscopy to observe the cellular events in both the periphery and central region of the 3D culture between day 3 and 4 of differentiation. EC sprouting and migration were observed in the peripheral region of the network (Fig. 8A, time-lapse movies are available in the Supplementary Movie S3). ECs extended dynamic filopodia to sense guidance cues, followed by body elongation and retraction, which drove them away from the pre-existing vessel; they migrated to the targets (Fig. 8B, 0–525 min, arrows). With the sprouting of ECs in the capillary front, ECs in the capillary rear divided to replenish cell number (Fig. 8B, 525 min, arrowhead). In the central area, we were able to observe the sequence of path finding and contact between an angiogenic sprout and its target vessel (Fig. 8C). Sprouting occurred as lateral outgrowths from pre-existing capillaries. Sprouting ECs had elongated filopodial extensions that behaved similar to an axon growth cone (Fig. 8D, 0.0–14.7 h, arrows). Along with vessel growth, small vacuoles appeared in the capillary rear and fused to form a luminal space within the capillary (Fig. 8D, 5.3–14.7 h, arrowheads; time-lapse movies and a rotating image of a 3D reconstruction are available in the Supplementary Movies S4 and S5). In addition to intracellular lumen formation, we observed intercellular slit-like lumenogenesis (Fig. 8E, time-lapse movies are available in the Supplementary Movie S6). In this case, 2 vessels simultaneously sprouted from a pre-existing capillary vessel. During sprouting, these vessels first twisted together, and then grew out in parallel to the target vessels (Fig. 8E, 0.0–14.0 h, arrows). After pathfinding behaviors, the lamellipodia and filopodia extensions (Fig. 8E, 0.0–6.0 h, arrowheads) generated by each vessel eventually fused to enclose a luminal space between these vessels (Fig. 8E, 8.0–14.0 h, asterisk). Taken together, a complex web of interconnected capillaries was formed by

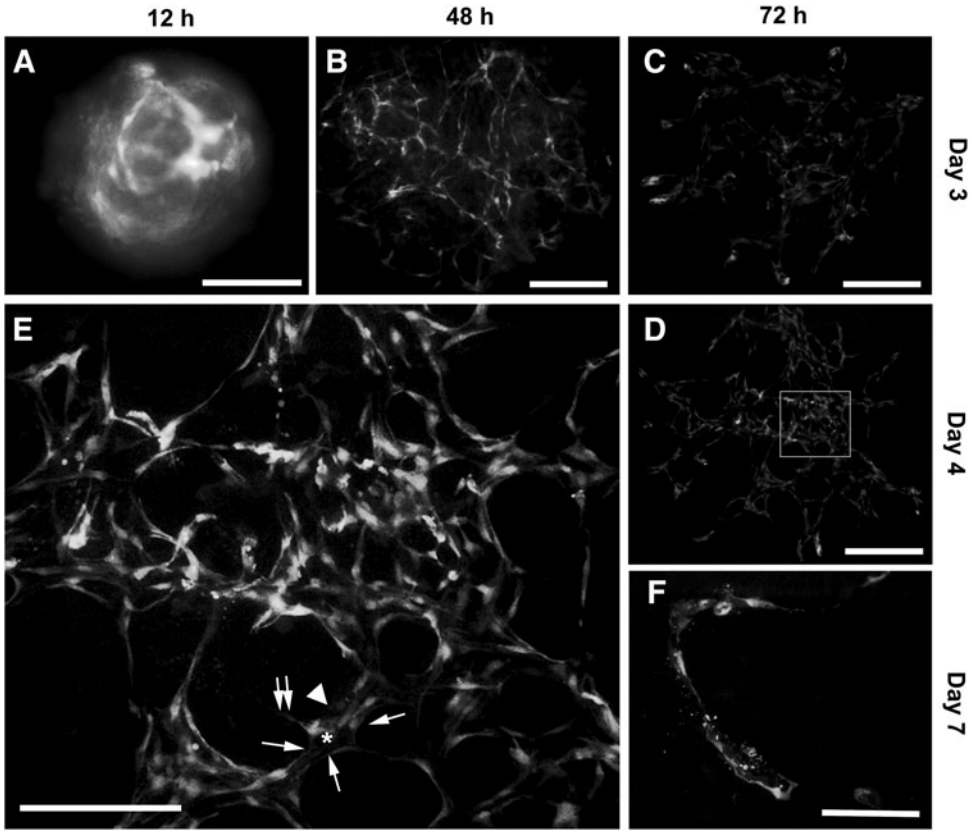

FIG. 5. Formation of the capillary network by ESC-ECs in aggregates embedded in the 3D collagen gel sandwich. **(A)** Aggregates seeded in the 3D collagen gel sandwich for 12 h. **(B)** ESC-ECs migrate out of the aggregates and form typical cord-like structures after 48 h. **(C)** Cord-like ECs coalesce into a primary vascular plexus on day 3. **(D)** The remodeling of the primary vascular plexus into a capillary network on day 4. **(E)** High-power magnification (100×) of the white rectangular area in D. *Arrowhead* indicates a representative capillary-like structure containing a lumen (*asterisk*) lined by 5–6 ECs (*arrows*). One of the lining ECs has abluminal filopodial extensions (*twin arrows*). **(F)** Collapse of the capillary network on day 7. Scale bars, 200 μm. 3D, 3-dimensional.

ECs through coordinated sprouting, migration, lumenogenesis, and anastamosis.

Discussion

Our study demonstrates that the in vitro ESC-EC angiogenesis model is a high-resolution, dynamic video-imaging system for long-term imaging of the cellular events that occur during angiogenesis; additionally, it could be used as a screening tool for the identification of novel pro-angiogenic and anti-angiogenic molecules. GFP expression was detected throughout the ESC-EC angiogenesis, enabling us to observe the membrane protrusions of the cells (e.g., filopodia and lamellipodia extensions) and intermediate state during the cell's morphological transitions, facilitating detailed analysis of the cellular processes that occur during angiogenesis. In this respect, these transgenic ESC-ECs provide a major advantage for observing the development of blood vessels over models that only permit light microscopic observations, which provide limited resolution. In addition, this model allows continuous observation of blood vessel development in real time, which is advantageous over discontinuous and non-real-time histological analysis. In comparison to other models for screening, these aggregates, which are composed of defined numbers of ESC-ECs, commonly display similar phenotypes outlined by green fluorescence within 3 days, thus rendering them easily accessible for automated computational data analysis.

The in vitro ESC-EC angiogenesis system provides an excellent opportunity for observing angiogenesis. In this model, vessels develop in a central to peripheral manner so that vessels at the migrating front of the developing vascular plexus are less mature, compared with more central vessels. Therefore, there is a spatial separation of different aspects of angiogenesis, such as EC sprouting and migration at the growing edge of the vascular plexus and vessel sprouting, lumenogenesis, and anastomosis at the more proximal vascular plexus. We have successfully performed time-lapse imaging using spinning disc confocal microscopy to record continuous EC morphogenesis for up to 24 h. This model allows for prolonged observation, demonstrating that in vitro ESC-EC angiogenesis bears striking resemblance to developmental angiogenesis in vivo. We find that ECs in the capillary front generate extensive filopodial extensions that integrate directional cues from their environment to define the direction in which the new sprout grows and create connections with adjacent sprouts to generate functional vascular networks. This phenomenon has been well documented in mouse retina angiogenesis [40–43] and are a hallmark of angiogenic blood vessels [40]. EC lumen development that involved the formation and fusion of intracellular vacuoles has been extensively reported in various in vivo and in vitro angiogenesis models [14,36,44]. We also observed the formation of small vacuoles in the capillary rear during vessel outgrowth, and these vacuoles fused to create a progressively larger luminal space. With the exception of intracellular vacuolation and lumen formation, we found ECs aligned around an intercellular space that was formed by lamellipodial and filopodial fusion in front of 2 sprouting vessels. This is consistent with the most recent study that the intersegmental vessel lumen in the zebrafish embryo is formed by the arrangement of ECs around an intercellular

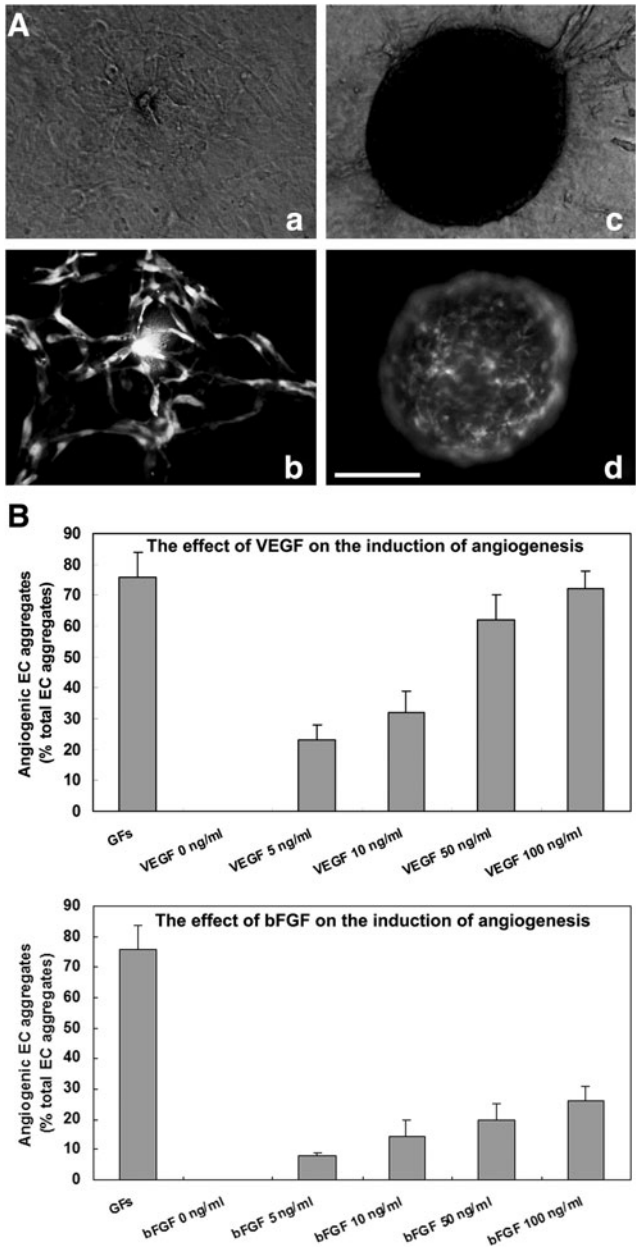

FIG. 6. The induction of ESC-EC angiogenesis by angiogenic CFs (VEGFs). **(A)** Representative pictures of the angiogenic aggregate **(a, b)** and nonangiogenic aggregate **(c, d)** 3 days after embedding in a 3D collagen gel sandwich; **(a, c)** in bright field; and **(b, d)** in fluorescence. **(B)** Quantitative analysis of the proportion of angiogenic aggregates after 72 h of basic fibroblast growth factor 2 (FGF2) or VEGF treatment. Nonangiogenic and angiogenic vascular phenotypes were scored among at least 96 aggregates in each experiment. Data are the mean ± SD of 3 independent experiments. Scale bar, 200 μm. VEGF, vascular endothelial growth factor.

luminal space [15]. According to various models of sprouting angiogenesis, ECs at the leading edge of vascular sprouts that generate filopodia extension are lumenless ECs called "tip cells," whereas the lumen-generating ECs in the capillary rear are known as "stalk cells" [41]; however, we could not distinguish the tip cells from the stalk cells during vessel sprouting in this model. Therefore, a more dedicated transgenic ESC line is required; ideally, this line would have labels for EC borders, nuclei, or membrane proteins to dissect the distinct steps of proliferation, vacuole formation and fusion, and lumen formation.

Korff and Augustin have shown that EC aggregates are a 2-compartment system consisting of a core of unorganized cells and a surface layer of cells that have a high degree of cellular quiescence [28]. We find that our ESC-EC aggregates have the same characteristics in that ECs switched from the quiescent state to become angiogenic in the presence of angiogenic stimulus; otherwise, ESC-ECs stayed in the aggregates with no signs of angiogenic growth. We used our model to test 2 angiogenic GFs. Compared with VEGF, which plays major roles in the induction of ESC-EC angiogenesis, the strong angiogenic agent FGF2 exhibited a minor contribution. This finding is in contrast to previous reports that both VEGF and FGF2 are required to induce EC angiogenesis in 3D collagen matrices, and when applied in combination, these 2 cytokines demonstrate synergism [45]. However, the conflicting data can be explained by the divergence of ECs used in different 3D models (e.g., we use capillary-like ESC-ECs, whereas others use adult or macrovascular ECs [35,36]) and the fact that ESC-EC angiogenesis bears striking resemblance to developmental angiogenesis. It has been reported that during embryonic development, VEGFA/VEGFR2 (vascular endothelial growth factor receptor 2, also known as F1K1/KDR)-dependent vessel formation occurs in the absence of FGF2/FGFR1 [46–49]. FGF2, by contrast, has been reported to act as a mitogen for both endothelial and mural cells and its role during embryonic vascular development are synergistic with VEGF in maintenance of the vascular integrity through PDGF-B–PDGFRβ signaling [50]. This could explain why VEGF-A is the dominating driving force in the induction of sprouting angiogenesis in this aggregate-based ESC-EC angiogenesis assay. Future plans include involving ESC-derived mural cells in this system to induce the tubule formation during which FGF2 is required to ensure the development of mature vessels. However, our system could be used to identify the role of molecules that affect ESC-EC angiogenesis, which have been highlighted in regenerative medicine as a cure for vascular disease.

In contrast to the 2D collagen monolayer culture, ESC-EC survival time was obviously prolonged under conditions that permit the aggregate–matrix contacts of both the upper and bottom layer of the aggregate. This indicates a crucial role for cell–matrix contacts in ESC-EC survival [51,52]. It is well known that the extracellular matrix acts as a morphogenic regulator and delivers an anti-death signal via integrin-mediated signaling [53–55]. Consistent with this, when a β1 integrin blocking antibody is applied, ESC-ECs have a significantly shortened survival time, even in the presence of high concentrations of VEGF. In spite of modulating EC survival, collagen matrix-integrin signaling also regulates cell migration [56,57]. Our 3D model displays the corresponding phenotypes (impaired migration and poor vascularization) upon integrin inhibition. The inhibition of β1 integrin perturbs the EC attachment to collagen. It has been reported that collagen I, the ligand of α1β1 and α2β1 integrins, exerts an inhibitory action on the tyrosine kinase receptor [58]. EC adhesion to collagen I reduces VEGF-A-induced VEGFR-2 autophosphorylation by recruiting the

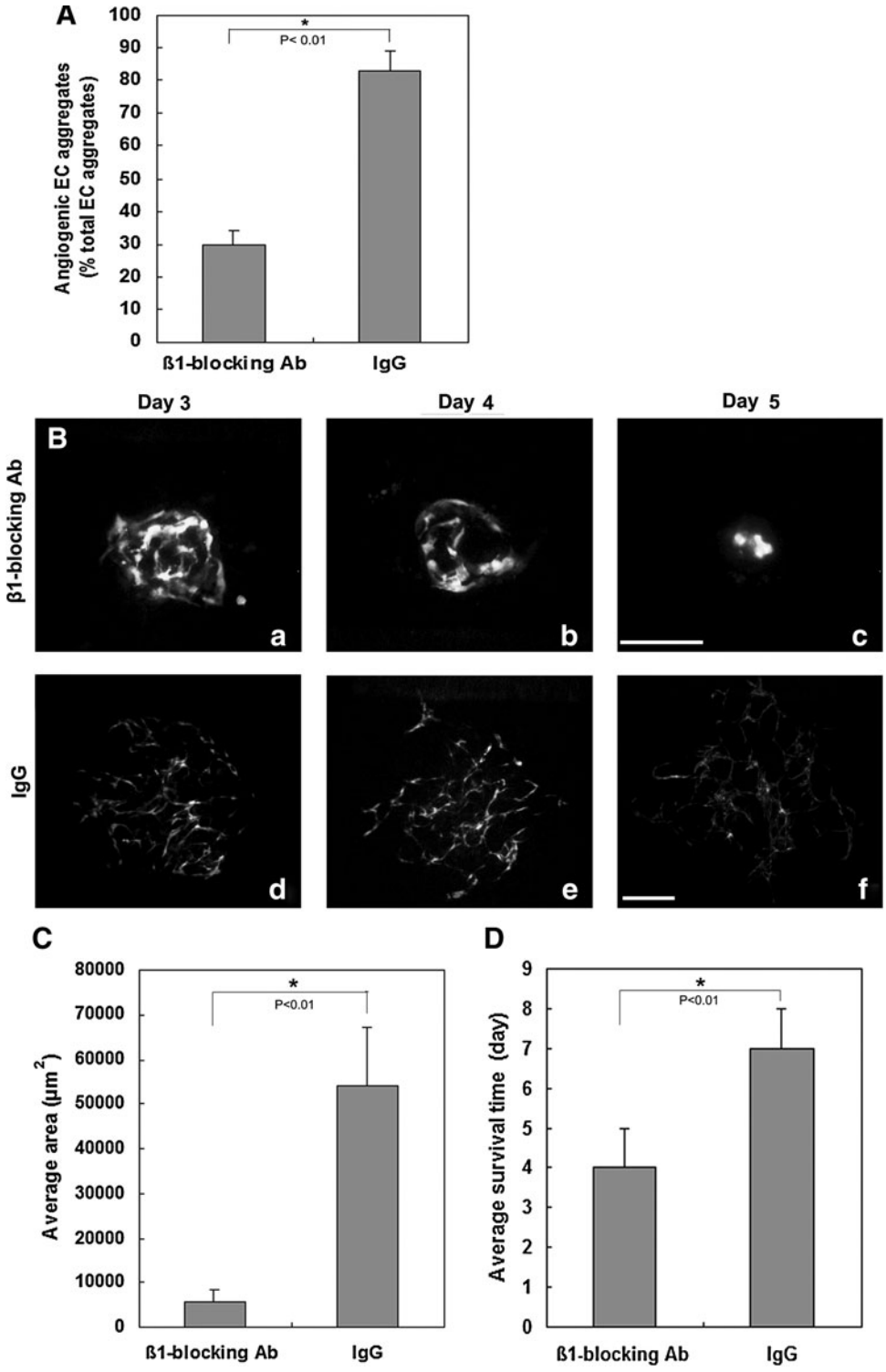

FIG. 7. Effects of the β1 integrin blocking antibody on ESC-EC angiogenesis. **(A)** Quantitative analysis of the proportion of angiogenic aggregates after 72 h of β1 integrin blocking. Non-angiogenic and angiogenic vascular phenotypes were scored among at least 96 ESC-EC aggregates. **(B)** The development of the angiogenic aggregate after β1 integrin blocking antibody treatment **(a–c)**; **(d–f)** IgG-treated control. **(C)** Quantitative analysis of the average vascularized area in day 3 angiogenic aggregates after β1 integrin blocking antibody treatment. **(D)** Quantitative analysis of the ESC-EC survival time in angiogenic aggregates after β1 integrin blocking antibody treatment. Data are the mean ± SD of 3 independent experiments. An *asterisk* (*) indicates a significant difference ($P < 0.01$). Scale bar, 200 μm.

tyrosine phosphatase SHP2 to the phosphorylated Tyr1117 of the receptor cytosolic tail. The inhibiting activity exerted by SHP2 on VEGFR-2 is strictly dependent on EC adhesion to collagen I and was crucial to allow an accurate response of ECs migrating along VEGF-A gradients [59]. We speculate that inhibition of integrin β1 perturbed the EC adhesion to collagen I and the subsequent VEGFR-2 internalization exerted by SHP2, inhibiting the subcellular localization of RTK signaling, which is the guidance for the EC migration. The exact signaling events need further investigation. However, the sensitivity to matrix modulation highlighted the ESC-EC aggregate-based model as a tool to investigate the tyrosine kinase receptors and integrin interactions.

Although our in vitro ESC-EC angiogenesis model cannot display the complete portrait of angiogenesis in vivo, it is one of the few that using an unlimited cell source ESCs,

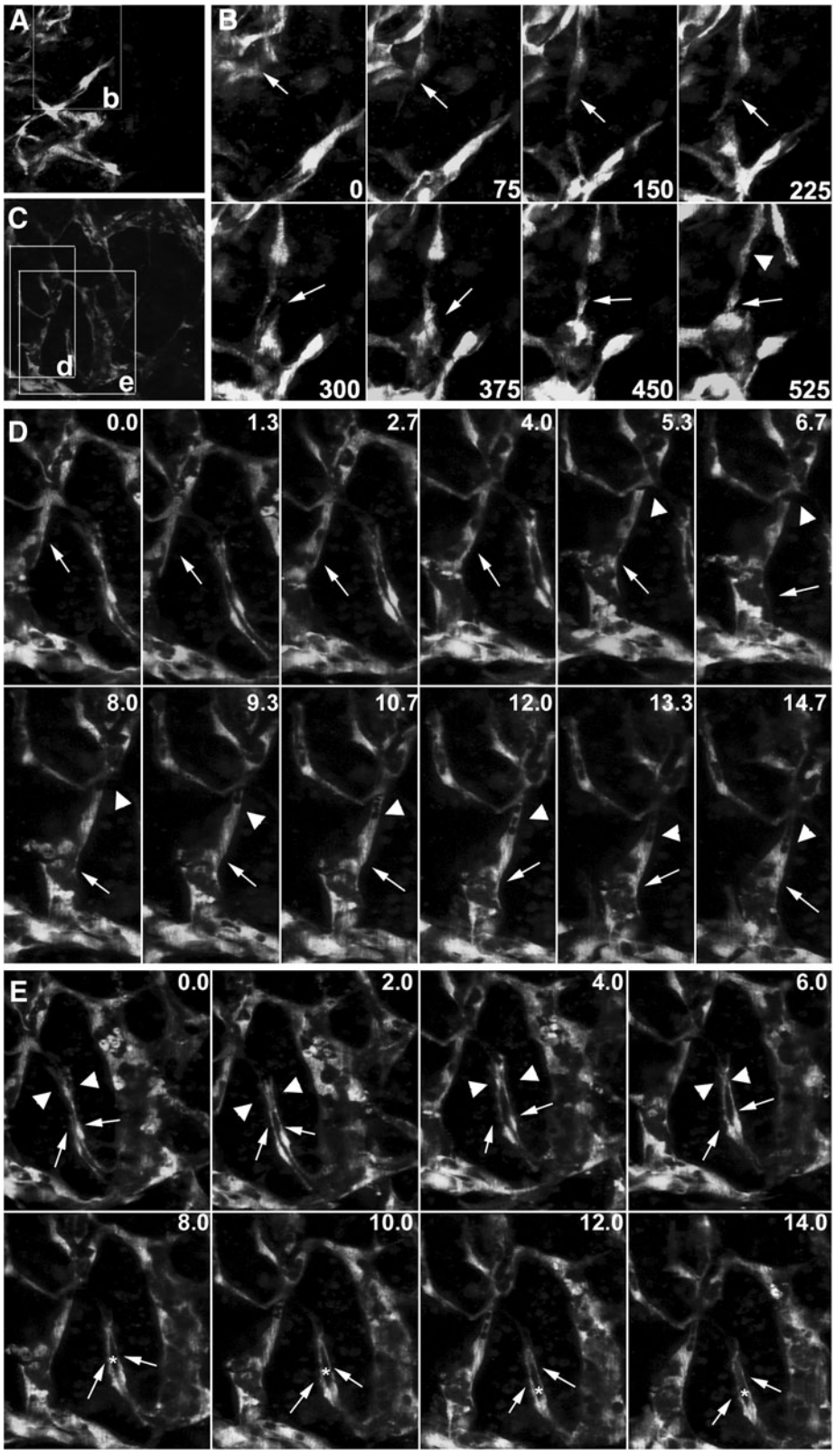

FIG. 8. Live imaging of the cellular events during ESC-EC angiogenesis in vitro. **(A)** The peripheral region of the capillary network. The boxed area labeled "**b**" indicates regions shown in **B**. **(B)** A sprouting vessel (*arrows* in time points exhibit extension and regression of the long filopodia during outgrowth; see Supplementary Movie S3). When the frontal EC migrated away from the previous vessels, cell division occurred in the capillary rear (*arrowhead* in time point 525 min). **(C)** The central area of the capillary network. The boxed areas labeled "**d**" and "**e**" indicate regions shown in **D** and **E**. **(D)** Lumen formation of a sprouting vessel. This vessel generates long filopodial extensions toward its targets (*arrows*). During its outgrowth, small vacuoles appear in the capillary rear, and the fusion of these vacuoles leads to a progressively larger lumen (*arrowheads* in time points 5.3–14.7 h, see Supplementary Movie S4). **(E)** Intercellular lumen formation in a vessel adjacent to the sprouting vessel in **D**. Two ECs (*arrows*) sprouting from the pre-existing vessel twist together, but with individual filopodia and lamellipodia extensions (*arrowheads* in time points 0.0–6.0 h), which then fuse to enclose a lumen (*asterisks* in time points 8.0–14.0 h) between 2 ECs (see Supplementary Movie S6). Scale bar, 200 μm.

which in most extent mimic the capillary EC angiogenesis during development; therefore, providing a platform for the study of molecules governing different steps of angiogenesis. By labeling candidate proteins with different colors, it may be possible to observe protein–protein interactions during a continuous cellular process. Considering its sensitivity to agents with anti-angiogenic and pro-angiogenic activity and that it displays synchronized phenotypes after treatment, it is also an ideal image screening tool for identification of novel pro- and anti-angiogenic compounds.

Acknowledgment

We thank Dr. Janet Rossant for generously providing Flk $1^{GFP/+}$ ESCs.

Author Disclosure Statement

No competing financial interests exist.

References

1. Folkman J and PA D'Amore. (1996). Blood vessel formation: what is its molecular basis? Cell 87:1153–1155.
2. Pang RW and RT Poon. (2006). Clinical implications of angiogenesis in cancers. Vasc Health Risk Manag 2:97–108.
3. Holderfield MT and CC Hughes. (2008). Crosstalk between vascular endothelial growth factor, notch, and transforming growth factor-beta in vascular morphogenesis. Circ Res 102:637–652.
4. De Smet F, P Carmeliet and M Autiero. (2006). Fishing and frogging for anti-angiogenic drugs. Nat Chem Biol 2:228–229.
5. Maas JW, FA Le Noble, GA Dunselman, AF de Goeij, HA Struyker Boudier and JL Evers. (1999). The chick embryo chorioallantoic membrane as a model to investigate the angiogenic properties of human endometrium. Gynecol Obstet Invest 48:108–112.
6. Norrby K. (2006). In vivo models of angiogenesis. J Cell Mol Med 10:588–612.
7. Balke M, A Neumann, C Kersting, K Agelopoulos, C Gebert, G Gosheger, H Buerger and M Hagedorn. (2010). Morphologic characterization of osteosarcoma growth on the chick chorioallantoic membrane. BMC Res Notes 3:58.
8. Ausprunk DH and J Folkman. (1977). Migration and proliferation of endothelial cells in preformed and newly formed blood vessels during tumor angiogenesis. Microvasc Res 14:53–65.
9. Bian F, MC Zhang and Y Zhu. (2008). Inhibitory effect of curcumin on corneal neovascularization in vitro and in vivo. Ophthalmologica 222:178–186.
10. Sharma A, DI Bettis, JW Cowden and RR Mohan. (2010). Localization of angiotensin converting enzyme in rabbit cornea and its role in controlling corneal angiogenesis in vivo. Mol Vis 16:720–728.
11. Akhtar N, EB Dickerson and R Auerbach. (2002). The sponge/Matrigel angiogenesis assay. Angiogenesis 5:75–80.
12. Kragh M, PJ Hjarnaa, E Bramm, PE Kristjansen, J Rygaard and L Binderup. (2003). In vivo chamber angiogenesis assay: an optimized Matrigel plug assay for fast assessment of anti-angiogenic activity. Int J Oncol 22:305–311.
13. Lawson ND and BM Weinstein. (2002). In vivo imaging of embryonic vascular development using transgenic zebrafish. Dev Biol 248:307–318.
14. Kamei M, WB Saunders, KJ Bayless, L Dye, GE Davis and BM Weinstein. (2006). Endothelial tubes assemble from intracellular vacuoles in vivo. Nature 442:453–456.
15. Blum Y, HG Belting, E Ellertsdottir, L Herwig, F Lüders and M Affolter. (2008). Complex cell rearrangements during intersegmental vessel sprouting and vessel fusion in the zebrafish embryo. Dev Biol 316:312–322.
16. Staton CA, MW Reed and NJ Brown. (2009). A critical analysis of current in vitro and in vivo angiogenesis assays. Int J Exp Pathol 90:195–221.
17. Go RS and WG Owen. (2003). The rat aortic ring assay for in vitro study of angiogenesis. Methods Mol Med 85:59–64.
18. Muthukkaruppan VR, BL Shinners, R Lewis, S-J Park, BJ Baechler and R Auerbach. (2000). The chick embryo aortic arch assay: a new, rapid, quantifiable in vitro method for testing the efficacy of angiogenic and anti-angiogenic factors in a three-dimensional, serum free organ culture system. Proc Am Assoc Cancer Res 41:65.
19. Nicosia RF, WH Zhu, E Fogel, KM Howson and AC Aplin. (2005). A new *ex vivo* model to study venous angiogenesis and arterio-venous anastomosis formation. J Vasc Res 42:111–119.
20. Jaffe EA, RL Nachman, CG Becker and CR Minick. (1973). Culture of human endothelial cells derived from umbilical veins. Identification by morphologic and immunologic criteria. J Clin Invest 52:2745–2756.
21. Davis GE, W Koh and AN Stratman. (2007). Mechanisms controlling human endothelial lumen formation and tube assembly in three-dimensional extracellular matrices. Birth Defects Res C Embryo Today 81:270–285.
22. Koh W, RD Mahan and GE Davis. (2008). Cdc42- and Rac1-mediated endothelial lumen formation requires Pak2, Pak4 and Par3, and PKC-dependent signaling. J Cell Sci 121:989–1001.
23. Jeong A, HJ Lee, SJ Jeong, HJ Lee, EO Lee, H Bae and SH Kim. (2010). Compound K inhibits basic fibroblast growth factor-induced angiogenesis via regulation of p38 mitogen activated protein kinase and AKT in human umbilical vein endothelial cells. Biol Pharm Bull 33:945–950.
24. Bai H, CD McCaig, JV Forrester and M Zhao. (2004). DC electric fields induce distinct preangiogenic responses in microvascular and macrovascular cells. Arterioscler Thromb Vasc Biol 24:1234–1239.
25. Silvestre JS, Lévy BI and A Tedgui. (2008). Mechanisms of angiogenesis and remodelling of the microvasculature. Cardiovasc Res 78:201–202.
26. Yamashita J, H Itoh, M Hirashima, M Ogawa, S Nishikawa, T Yurugi, M Naito, K Nakao, and S Nishikawa. (2000). Flk1-positive cells derived from embryonic stem cells serve as vascular progenitors. Nature 408:92–96.
27. Yamahara K, M Sone, H Itoh, JK Yamashita, T Yurugi-Kobayashi, K Homma, TH Chao, K Miyashita, K Park, N Oyamada, N Sawada, D Taura, Y Fukunaga, N Tamura and K Nakao. (2008). Augmentation of neovascularization [corrected] in hindlimb ischemia by combined transplantation of human embryonic stem cells-derived endothelial and mural cells. PLoS ONE 3:e1666.
28. Korff T and HG Augustin. (1998). Integration of endothelial cells in multicellular spheroids prevents apoptosis and induces differentiation. J Cell Biol 143:1341–1352.
29. Korff T and HG Augustin. (1999). Tensional forces in fibrillar extracellular matrices control directional capillary sprouting. J Cell Sci 112:3249–3258.
30. Vlodavsky I, J Folkman, R Sullivan, R Fridman, R Ishai-Michaeli, J Sasse and M Klagsbrun. (1987). Endothelial cell-derived basic fibroblast growth factor: synthesis and deposition into subendothelial extracellular matrix. Proc Natl Acad Sci USA 84:2292–2296.
31. Folkman J and Y Shing. (1992). Angiogenesis. J Biol Chem 267:10931–10934.
32. Krah K, V Mironov, W Risau and I Flamme. (1994). Induction of vasculogenesis in quail blastodisc-derived embryoid bodies. Dev Biol 164:123–132.
33. Mattern J, R Koomägi and M Volm. (1997). Coexpression of VEGF and bFGF in human epidermoid lung carcinoma is associated with increased vessel density. Anticancer Res 17:2249–2252.

34. Kiec-Wilk B, J Grzybowska-Galuszka, A Polus, J Pryjma, A Knapp and K Kristiansen. (2010). The MAPK-dependent regulation of the Jagged/Notch gene expression by VEGF, bFGF or PPAR gamma mediated angiogenesis in HUVEC. J Physiol Pharmacol 61:217–225.
35. Senger DR, CA Perruzzi, M Streit, VE Koteliansky, AR de Fougerolles and M Detmar. (2002). The alpha(1)beta(1) and alpha(2)beta(1) integrins provide critical support for vascular endothelial growth factor signaling, endothelial cell migration, and tumor angiogenesis. Am J Pathol 160:195–204.
36. Davis GE and KJ Bayless. (2003). An integrin and Rho GTPase-dependent pinocytic vacuole mechanism controls capillary lumen formation in collagen and fibrin matrices. Microcirculation 10:27–44.
37. Avraamides CJ, B Garmy-Susini and JA Varner. (2008). Integrins in angiogenesis and lymphangiogenesis. Nat Rev Cancer 8:604–617.
38. Gullberg D, KR Gehlsen, DC Turner, K Ahlén, LS Zijenah, MJ Barnes and K Rubin. (1992). Analysis of alpha 1 beta 1, alpha 2 beta 1 and alpha 3 beta 1 integrins in cell—collagen interactions: identification of conformation dependent alpha 1 beta 1 binding sites in collagen type I. EMBO J 11:3865–3873.
39. Leitinger B and E Hohenester. (2007). Mammalian collagen receptors. Matrix Biol 26:146–155.
40. Cleaver O and PA Krieg. (1999). Molecular mechanisms of vascular development. In: *Heart Development*. Harvey RP, Rosenthal N, eds. Academic Press, San Diego, pp 221–252.
41. Gerhardt H, M Golding, M Fruttiger, C Ruhrberg, A Lundkvist, A Abramsson, M Jeltsch, C Mitchell, K Alitalo, D Shima and C Betsholtz. (2003). VEGF guides angiogenic sprouting utilizing endothelial tip cell filopodia. J Cell Biol 161:1163–1177.
42. Isogai S, ND Lawson, S Torrealday, M Horiguchi and BM Weinstein. (2003). Angiogenic network formation in the developing vertebrate trunk. Development 130:5281–5290.
43. Hellström M, LK Phng, JJ Hofmann, E Wallgard, L Coultas, P Lindblom, J Alva, AK Nilsson, L Karlsson, N Gaiano, K Yoon, J Rossant, ML Iruela-Arispe, M Kalén, H Gerhardt and C Betsholtz. (2007). Dll4 signalling through Notch1 regulates formation of tip cells during angiogenesis. Nature 445:776–780.
44. Davis GE, KJ Bayless and A Mavila. (2002). Molecular basis of endothelial cell morphogenesis in three-dimensional extracellular matrices. Anat Rec 268:252–275.
45. Kano MR, Y Morishita, C Iwata, S Iwasaka, T Watabe, Y Ouchi, K Miyazono and K Miyazawa. (2005). VEGF-A and FGF-2 synergistically promote neoangiogenesis through enhancement of endogenous PDGF-B-PDGFRbeta signaling. J Cell Sci 118:3759–3768.
46. Ozaki H, N Okamoto, S Ortega, M Chang, K Ozaki, S Sadda, MA Vinores, N Derevjanik, DJ Zack, C Basilico and PA Campochiaro. (1998). Basic fibroblast growth factor is neither necessary nor sufficient for the development of retinal neovascularization. Am J Pathol 153:757–765.
47. Ortega S, M Ittmann, SH Tsang, M Ehrlich and C Basilico. (1998). Neuronal defects and delayed wound healing in mice lacking fibroblast growth factor 2. Proc Natl Acad Sci USA 95:5672–5677.
48. Feraud O, Y Cao and D Vittet. (2001). Embryonic stem cell-derived embryoid bodies development in collagen gels recapitulates sprouting angiogenesis. Lab Invest 81:1669–1681.
49. Magnusson P, C Rolny, L Jakobsson, C Wikner, Y Wu, DJ Hicklin and L Claesson-Welsh. (2004). Deregulation of Flk-1/vascular endothelial growth factor receptor-2 in fibroblast growth factor receptor-1-deficient vascular stem cell development. J Cell Sci 117:1513–1523.
50. Kano MR, Y Morishita, C Iwata, S Iwasaka, T Watabe, Y Ouchi, K Miyazono and K Miyazawa. (2005). VEGF-A and FGF-2 synergistically promote neoangiogenesis through enhancement of endogenous PDGF-B-PDGFRbeta signaling. J Cell Sci 118:3759–3768.
51. Chavakis E and S Dimmeler. (2002). Regulation of endothelial cell survival and apoptosis during angiogenesis. Arterioscler Thromb Vasc Biol 22:887–893.
52. Stephan S, SG Ball, M Williamson, DV Bax, A Lomas, CA Shuttleworth and CM Kielty. (2006). Cell-matrix biology in vascular tissue engineering. J Anat 209:495–502.
53. Friedrich EB, E Liu, S Sinha, S Cook, DS Milstone, CA MacRae, M Mariotti, PJ Kuhlencordt, T Force, A Rosenzweig, R St-Arnaud, S Dedhar and RE Gerszten. (2004). Integrin-linked kinase regulates endothelial cell survival and vascular development. Mol Cell Biol 24:8134–8144.
54. Davis GE and DR Senger. (2008). Extracellular matrix mediates a molecular balance between vascular morphogenesis and regression. Curr Opin Hematol 15:197–203.
55. Zhao J, Y Zhang, SS Ithychanda, Y Tu, K Chen, J Qin and C Wu. (2009). Migfilin interacts with Src and contributes to cell-matrix adhesion-mediated survival signaling. J Biol Chem 284:34308–34320.
56. Moissoglu K and MA Schwartz. (2006). Integrin signalling in directed cell migration. Biol Cell 98:547–555.
57. Shattil SJ, C Kim and MH Ginsberg. (2010). The final steps of integrin activation: the end game. Nat Rev Mol Cell Biol 11:288–300.
58. Mitola S, B Brenchio, M Piccinini, L Tertoolen, L Zammataro, G Breier, MT Rinaudo, J den Hertog, M Arese and F Bussolino. (2006). Type I collagen limits VEGFR-2 signaling by a SHP2 protein-tyrosine phosphatase-dependent mechanism 1. Circ Res 98:45–54.
59. Jékely G, HH Sung, CM Luque and P Rørth. (2005). Regulators of endocytosis maintain localized receptor tyrosine kinase signaling in guided migration. Dev Cell 9:197–207.

Address correspondence to:
Dr. Jia Li
Med-X-Renji-Clinical Stem Cell Institute
Renji Hospital
Shanghai Jiaotong University Medical College
1678 Dongfang Road
Shanghai 200127
China

E-mail: jil2012@med.cornell.edu; msunlijia@msn.com

Received for publication December 26, 2010
Accepted after revision March 8, 2011
Prepublished on Liebert Instant Online March 8, 2011